FR-1816

NAVAL RESEARCH LABORATORY REPORT

27 November 1941

THE USE OF PLASTIC MODELS IN ELASTIC STUDIES
(A STUDY OF THE AIRCRAFT CARRIER BENT MODELS)

By

H. B. Maria

Report No. R-1816

NAVY DEPARTMENT
OFFICE OF NAVAL RESEARCH
NAVAL RESEARCH LABORATORY
WASHINGTON 20, D. C.

27 November 1941

NRL Report No. H-1816

NAVY DEPARTMENT

Report of Test

on

The Use of Plastic Models in Elastic Studies

(A Study of the Aircraft Carrier Bent Models)

NAVAL RESEARCH LABORATORY
ANACOSTIA STATION
WASHINGTON, D. C.

Number of Pages: Text - 11 Tables - 10 Plates - 13

Authorization: Request of Commander W. P. Roop, David Taylor Model Basin.

Date of Test: October - November 1941.

Tests conducted by: H. B. Maris

H. B. Maris, Physicist

J. S. Brock

J. S. Brock, Contract Employee

Reviewed by: E. O. Hulburt

E. O. Hulburt, Head Physicist

Approved by: H. G. Bowen

H. G. Bowen, Rear Admiral, USN. Director

Distribution: BuShips (10)

ect

TABLE OF CONTENTS

APPENDICES

TABLE OF CONTENTS (Continued)

APPENDICES

AUTHORIZATION

1. The following report was written at the request of Commander W. P. Roop of the David Taylor Model Basin.

PLAN

2. Dr. L. C. Maugh from the University of Michigan was on a ten day assignment at the David Taylor Model Basin with the purpose of demonstrating the Begg's method of analyzing indeterminate elastic structures.

3. J. S. Brock and H. B. Maris from the Naval Research Laboratory were detailed to assist Dr. Maugh in the preparation of models and obtaining materials and instruments for the tests.

4. The aircraft carrier Bent was selected as a demonstration problem. Plans were made for the testing of three different knee designs made of two different materials, a total of six different models as shown in Plate 1.

Purpose

5. The purpose of the plan was to demonstrate the efficiency and convenience of plastic models for use in elastic studies. The work of making and assembling the models was therefore a part of the demonstration.

6. DuPonts, Plastacele, a cellulose acetate, and a Rohm & Haas Lucite, a methyl-methacrylate, were selected for the model materials. Plastacele was selected because it is tough and easy to work. Plexiglas, which is much more brittle and therefore much more difficult to fabricate, was selected because it is very free from warping and generally has better elastic properties after the models are built.

7. G. Y. McDaniels, the machinist assigned to the work, remarked when he got the assignment that he should never have been assigned to a rush job. He was shop steward, in charge of the cafeteria, and had several other general duties. He began work the morning of the third day and spent between four and five days' time cutting out the six models. Since this was his first experience with machining either plastacele or plexiglas it is obvious that better time could be made with experience. About one day's time was lost by mistakes made due to inexperience and efforts to speed the work.

8. The cut materials were cemented into the models shown in Plate 1 by the laboratory personnel. Experience at the Research Laboratory has shown that this work can be done better by the shop force

but the ten days' limit to Dr. Maugh's assignment did not permit time for training shop personnel in this work.

9. These details of shop work are offered to emphasize the convenience and economy of plastic models for elastic study.

METHODS OF ANALYSIS (By Dr. Maugh)

(a) Use of the Reciprocal Theorem

10. The application of the Maxwell-Mohr Reciprocal Theorem will frequently provide the most convenient method for the determination of redundant forces, either external or internal in a statically indeterminate structure. This theorem will be explained in terms of the problems and models that form the basis of this report. For instance, the two hinged bent that is shown in Figure A of Plate 2 is statically indeterminate to the first degree as the horizontal reaction H_a is a redundant quantity. This quantity can, of course, be calculated by mathematical methods if assumptions are made in regard to the deformation of the material. These assumptions are usually not accurate in regard to the deformation in the material at the corners. To avoid the necessity of making such assumptions the value of H_a can be determined experimentally in the following manner:

11. Apply a force H' (Figure B of Plate 2) to the structure, or rather a small scale model of the structure, so as to cause the displacements shown by the broken line. Then, by the Reciprocal Theorem, the work done by the forces in Figure A of Plate 2, acting through the displacements caused by the forces in Figure B of Plate 2, is equal to the work done by the forces in Figure B of Plate 2 acting through the displacements in Figure A of Plate 2, or

$$-H_a \Delta_a + P_1 y_1 - P_2 y_2 - P_3 y_3 + \cdots = H' \, 0 = 0$$

or

$$H_a = + \frac{P_1 y_1}{\Delta_a} - P_2 \frac{y_2}{\Delta_a} - \frac{P_3 y_3}{\Delta_a} + \cdots \qquad (1)$$

12. Equation (1) shows that the reaction H_a due to any desired force system can be obtained by measuring the displacements y and Δ_a due to an auxiliary force system H'. The value of the auxiliary force H' is not involved but it is important that the auxiliary forces have no corresponding displacements caused by the actual forces. That is, the right hand side of the equation must be zero. On the tests that have been included in this report, the displacements y and Δ_a were measured with microscopes. The scale of the model does not enter into these results as the ratio $\frac{y}{\Delta}$ is independent of dimensions.

13. The same procedure can be used for fixed end bents such as Figure C of Plate 2 provided the proper auxiliary forces are used. For instance, if the horizontal reaction H_a is to be determined, the auxiliary forces shown in Figure D of Plate 2 must be used. These forces must give a horizontal movement Δ_h and prevent any vertical motion or rotation. This action is, of course, more difficult to obtain than in the first case, when the ends were free to rotate. However, the equations are identical, that is

$$H_a = P_1 \frac{y_1}{\Delta_h} - \frac{P_2 y_2}{\Delta_h} - \frac{P_3 y_3}{\Delta_h} + \text{---} \qquad (2)$$

14. Now if the model is given a vertical motion at a without horizontal movement or rotation as in Figure E of Plate 2, the reciprocal theorem gives

$$V_a \Delta_v + P_1 y_1 - P_2 y_2 - P_3 y_3 = 0$$

or

$$V_a = -P_1 \frac{y_1}{\Delta_v} + P_2 \frac{y_2}{\Delta_v} + \frac{P_3 y_3}{\Delta_v} + \text{---} \qquad (3)$$

This type of loading was not applied in the tests as will be explained later.

15. If the model is given a rotation θ_a at a without vertical or horizontal movement, as in Figure F of Plate 2, then

$$M_a \theta_a - P_1 y_1 - P_2 y_2 + P_3 y_3 = 0$$

or

$$M_a = P_1 \frac{y_1}{\theta a} + P_2 \frac{y_2}{\theta a} - P_3 \frac{y_3}{\theta a} + \text{---} \qquad (4)$$

Equation (4) involves the ratio of a linear displacement and an angle in radians and, therefore, the scale of the model affects the value. That is, the moments in the prototype will be n times the moments in the model where n is the scale ratio of dimensions. This procedure was used in determining the effects of different types of corners upon the forces acting on the frame. These tests and results will be described later.

(b) Use of Known Force Systems on Loaded Models

16. The determination of external forces by use of the reciprocal theorem is usually a comparatively simple procedure and, for the bents described in this report, gives all the information necessary

for calculating the shears and moments at any section. However, many structures are more redundant with respect to internal forces than external and in such cases, although the reciprocal theorem applies, it is not always easy to use. The stiffness of the structure cannot be determined except through the measurement of both forces and displacements. For this reason, the direct application of a load P (Figure G of Plate 2) and measurements of the displacement and rotations at various points may be desirable or necessary. Often in the analysis of continuous frame structures the theoretical calculations can be made with greater accuracy if the constants that relate the internal forces with the displacements are determined experimentally rather than computed. The measurement of displacements for any desired loading condition can also be used to show the relative stiffness of various types of structural details.

17. All models were tested by applying a concentrated load P at the center of the span. The value of the displacement Δ and the rotations θ_b and θ_c were measured by means of microscopes. These measurements serve to show the effect of the type of corner upon the stiffness of the structure. At the same time, the coefficients or constants for the members ab and cd can be obtained. As the value of H is known from the first test, by the reciprocal theorem, the relation between the end moment M_{ba} acting on the member ba and the rotation θ_b can be obtained.

$$M_{ba} = C_{ba}\,\theta_b = H_h \quad \text{or} \quad C_{ba} = \frac{H_h}{\theta_b} \tag{5}$$

The coefficients for members bc cannot be determined by this type of loading as the moment M_{bc} must be expressed in the form

$$M_{bc} = C_1\,\theta_b + C_2\,\theta_c + M_{fbc} \tag{6}$$

However, if the type of loading shown in Figure H of Plate 2 is used, then the coefficients for member bc can be determined.

$$\begin{aligned} M_{bc} &= C_1\,\theta_b + C_2\,\theta_c = H_a\,h - \frac{Ph}{2} \\ M_{cb} &= C_2\,\theta_b + C_1\,\theta_c = H_d\,h = (P - H_a)\,h \end{aligned} \tag{7}$$

18. The values of C_1 and C_2 can be obtained as the quantities H_a and H_d were obtained in the first test.

19. In the models that were tested, direct loads (both vertical and horizontal) were used to test the relative stiffness of

the various types of corners rather than the determination of coefficients. In general the value of coefficients for structural members can be obtained better by tests on separate models of the various members. The type of loading shown in Figure H of Plate 2 was not used in the tests.

20. The interpretation or use of displacement measurements that are obtained from the application of loads to small scale models in predicting the relative stiffness of large scale structures should be made with considerable judgment and care. That part of the displacement that is produced by general elastic deformation in the various members when adjusted by the scale ratio can, of course, be used without question. However, any local deformation in a zone that undergoes stress beyond the elastic range may not cause displacement for different scale ratios in the same degree as the elastic action. Some difference could be caused, of course, by the difference in local effect as at a sharp corner in small scale models. However, for the models tested, certain results that will be given later are definite while some must be used with caution. A corollary of the above statements would be that the avoidance of local concentrations by more gradual transition of cross-section produces more consistent and predictable elastic displacements.

MODELS STUDIED

21. Photographs of the six models studied are shown in Plate 1. For the plastacele models on the left .073 inch sheet was used for the web and .104 thickness strip for the flanges. For the lucite models on the right .060 inch sheet was used for the web and .080 thickness strips for the flanges. The flanges were 0.8 inch wide, the legs were 2.25 inches on the outside and the main beam 3.19 inches on the outside. The overall length was 42.25 inches. The depth from the top of the bent to the point of support was 13.25 inches. Youngs modulus is 2.19×10^5 pounds per square inch for plastacele and 3.86×10^5 for lucite. The plastacele was cemented with acetone and the lucite with methyl-ethyl-ketone. The acetone was used for the plastacele because it is quick setting and easy to work with. Acetic acid will make a stronger joint but it is slower in hardening. The stiffeners shown in all models were made from the web material.

22. Plate 8 shows the general layout of model L-3 on the work table ready for the tests. The two legs were held by pivots at the centers of each leg and 13.25 inches on the axis of the leg from the top line of the bent. The model is held free from friction with the table by ball bearings placed in small retaining cups.

23. The shackel for carrying the central load is seen near the center of the span and in line with it is the ball bearing pulley for directing the loading line. Plate 10 shows the model with the

center load applied and the reading microscope in position for reading the central deflection. It is to be noted that in Plate 10 the center span load is applied while the pivoted end supports are clamped to prevent rotation.

24. The pivot on the left in Plate 8 was designed as fixed while the pivot on the right was adjustable for the different types of displacement measurements. Plate 9 shows the detailed arrangement of the adjustable pivot. A brass collar a was forced into the celluloid base of the leg for a pressure fit to minimize play. This brass collar fit over the steel pivot b for a very neat fit, less than .001 inches play. The pivot was soldered to a flat bar c which was held in guides d on either side to prevent rotation or axial displacement while allowing normal displacement. The bar c carried two spacing blocks e, see also Plate 8. Wedges f between d and e held pivot b rigidly in place. Opposite wedges f spacing blocks g held the pivot accurately in any desired predetermined position. Changes in the spacing blocks gave the pivot any desired shift.

25. This use of spacing blocks between fixed shoulders, one fixed to the table d, and the other fixed to the pivot e, proved very satisfactory. It was found possible to return the pivot to any desired position with an accuracy of $\pm$ .001 inch.

26. Rotations of the bent leg about pivot b were either measured or prevented by bar h which was securely bolted to the base of the leg as shown. The distance from the center of pivot b to a dot on target i measured the radius of rotation while normal displacement of the dot with changes of the spacers g gave the amount of rotation. A similar bar on the left leg of the bent (see Plate 8) was free to move for hinged joint measurements but was rigidly attached to the table for the fixed end experiments.

27. Plate 10 shows model L3 arranged for the measurement of normal displacement with a known load on the center of the span. In this figure the ends of the bent are fixed.

28. Plate 11 shows the same model loaded with a tangential load in line with the top of the bent to simulate the load in a bent resulting from rolling of the ship. In this figure as in Plate 10 the joints are fixed.

29. Plate 12 shows model L3 arranged for measurement of knee rotation with a known load on the center of the span. Pointer k is mounted on block m which is rigidly attached to the web on the center line of the knee. Tangential movement of two targets on either end of pointer k are read by the two microscopes. The difference of the two readings measures the rotation.

MEASUREMENTS MADE

30. Tables 1-9 show in reduced form the data which were taken. The following tests were made on the various models.

31. (A) One leg of the models was given a fixed displacement as shown in Plate 11 and the following measurements were made: The displacements of the stations as shown in Plate 8 were noted for both hinged (Table 1) and fixed (Table 5) end conditions. Also the corner rotation (Table 6) was measured (Plate 12) for fixed ends. Both displacements and rotations were measured by traveling microscopes as described previously. Readings were taken to 0.0001 inch. Repeat settings were made until the values of displacements checked to less than 0.001 inch. The displacement of the leg was obtained by moving it first to one side of the neutral position and then to the other. In this manner comparatively large displacements were obtained with comparatively low values of stress. This reduced errors due to creep to a minimum. The tables show the displacements and rotations due to a unit displacement of the leg, that is, all displacements were divided by the distance through which the zero station moved.

32. (B) Vertical loads of 5, 15 and 35 pounds were applied at the midspan of the various models and the corresponding midspan deflections was measured for both hinged (Table 2) and fixed (Table 7) ends. Also the corner rotations were noted for hinged ends (Table 3) for the same type of load. These displacements and rotations are given in inches and radians respectively.

33. (C) Lateral loads of 5 and 10 pounds were applied and the side sway of the bent models was measured (Table 4). Due to the stiffness of the plexiglas models, loads of 20 pounds were applied in the case of fixed ends in order to obtain large deflections.

34. (D) One leg of the models was given a fixed rotation and the displacements of the various stations were measured for both hinged (Table 8) and fixed (Table 9) ends. The figures shown in these tables are the displacements of the various stations due to a rotation of the leg of one radian or the measured displacement divided by the measured rotation. These numbers are therefore the (y/θ) ratio of Equation 4 and may be used to calculate end moments. As an illustration suppose one wants to know the moment required to prevent the rotation of the hinged end bent leg due to a single load $\underline{w}$ acting at Station 6. From Table 8 (y/θ) is 1.05, 1.47, 1.13, respectively, for models C-1, C-2, and C-3 and the required moments would be 1.05 w, 1.47 w, and 1.13 w.

DISCUSSION OF DATA AND CURVES

35. The top of Plate 3 shows the influence lines or elastic curves for all models having hinged ends with one end subject to a fixed displacement. It will be clear that the displacements shown are greatly exaggerated. These curves are derived from the data of Table 1. The

displacements shown are the ratio of the motion of the point on the center line of the bent model to that of the leg. They may be used directly to calculate the horizontal reaction at the base of the bent due to a load placed anywhere on the bent by equation (1). Thus the horizontal reaction at the base of the model due to a load w placed at the midspan would be 0.296 w, 0.319 w and 0.334 w for models C-1, C-2 and C-3, respectively, as shown by Table 1. The corresponding values for models L-1, L-2 and L-3 are 0.275 w, 0.300 w, 0.340 w, respectively.

36. The curves at the left of Plate 4 show the midspan deflection as a function of the load at that point for hinged ends. For the models tested the magnitude of the deflection is a linear function of the applied load. The deflections for a 35 pound load was 0.1706", 0.1571" and 0.1388" (Table 2) for models C-1, C-2 and C-3, respectively. Corresponding values for models L-1, L-2 and L-3 was 0.1130", 0.0999" and 0.0847", respectively. The midspan deflection for the plastacele model with a square knee was 23% greater than the corresponding deflection for the plastacele model with a round knee. The plexiglas models show the same general difference in stiffness. The difference between the square and round knees in the latter case was 33%.

37. Plate 5 shows the corner rotation of the various models with hinged ends as a function of the load applied at the center of the span. The average value of the corner rotation for model C-1 was 0.00764 radians (Table 3) due to a load of 35 pounds. This is 16% more than the corresponding value (0.00604 radians) for model C-3 with round corners. Model L-1 shows a corner rotation of 0.00492 radians while model L-3 shows a value of 0.00359 radians. The difference in this case is 37%. Thus the midspan deflection and corner rotation show appreciable differences between the square and round corner knees. In each case the diagonal knee has shown intermediate values which are given and shown in the data and curves respectively.

38. Plate 6 shows the side sway of the bent models due to lateral loads for both hinged and fixed ends. The side sway for model C-1 (0.0694") was twice as much as for model C-3 (0.0347") for a load of 10 pounds with hinged ends as shown in Table 4. Model L-1 showed 57% (0.0496") more side sway than model L-3 (0.0315") for the same conditions of loading. A lateral load of 10 pounds is equivalent to the lateral thrust which would be given by a 35 pound load if the bent was subject to a roll of 17°. The side sway for model C-1 (0.0171") was 13% more than that for model C-3 (0.0151") for a load of 10 pounds with fixed ends while model L-1 showed 11% (0.0287") more side sway than model L-3 (0.0258") for a load of 20 pounds.

39. The bottom of Plate 3 shows the influence lines for all models having fixed ends with one end subject to a fixed displacement. These curves derived from Table 5 are magnified forms of the elastic curves of the bent models.

40. The right side of Plate 4 shows the midspan deflection of the various models as a function of the load applied to the bent models with fixed ends. The magnitude of these deflections is about the same as those for the models with hinged ends. Span strength is therefore affected very little by the anchorage of the legs. This is not true of the strength of the bent as a whole. The midspan deflection of model C-1 (0.1535") was 19% more than that for model C-3 (0.1281") and the deflection of model L-1 (0.1096") was 31% more than that for model L-3 (0.0835").

41. The maximum fiber stress was calculated at midspan from the deflection measurements due to a 35 pound load for both hinged and fixed end conditions and the results of this calculation is shown in Table 10, Column 3. For the hinged end condition Model C-1 showed a maximum midspan fiber stress of 621 pounds per square inch which was 10% more than for model C-3 (566 #/in^2). Model L-1 showed a maximum fiber stress of 754 #/in^2 which was 13% more than model L-3 (667 #/in^2). For the fixed end condition model C-1 showed a maximum midspan fiber stress of 595 #/in^2 as compared to 545 #/in^2 for model C-3. Model L-1 showed a maximum fiber stress of 744 #/in^2 which was 12% more than for model L-3 (664 #/in^2). Column 4 gives the midspan load that would be required to produce a maximum fiber stress of 2000 #/in^2 which is the assumed allowable working stress for these plastics. These data indicate that the span strength is increased at least 10% in the change from the square to round corner. This is not a measure of the strength of the bent as a whole for the bent would probably fail due to stress concentration in the web near the knee, and this would be much greater for the square knee than for the round one.

42. The top of Plate 7 shows the influence lines for all models with hinged ends due to a fixed rotation of one of the legs. The influence lines are the elastic curves derived from Table 8 of the various models in exagerated form.

43. The bottom of Plate 7 shows the influence lines, derived from Table 9, for all models with fixed ends due to a fixed rotation of one leg. No data was taken for model C-1. The vertical motion without horizontal movement or rotation as shown in Figure E of Plate 2 was not applied in this investigation due to the fact that this is a demonstration problem. In a problem of this nature all possibilities should be mentioned but not necessarily exhausted.

IDEALIZED BENTS OR EQUIVALENT TRUSSES

44. Plate 13 shows in diagram A and B two trusses designed to represent two solutions of the problem of the model aircraft carrier Bent discussed in the preceding paragraphs. In both diagrams the dimensions are held within those of the original model. The weight in each case is equal to that of the original model without the stiffeners. The diagrams show designs so planned that all members will be subjected to equal stress

by a normal load applied at the center of the span. The inner angle of each truss is 3.75 inches down and 3.125 inches in from the corner. This point is shown by the dotted lines of diagram B to be just inside the inner angle outline of both models 2 and 3.

45. Diagram A shows one half of an idealized hinged joint span. The base pivot is the same as with the models tested. A center span pivot is placed in line with the top of the bent.

46. Diagram B shows one half of a fixed end span. The spread at the points of support is the same as the spread of the flanges for the models tested.

47. The purpose of these two truss diagrams is to present a measure of the efficiency of the bent models tested. Theoretically the longest member under compression, 2 in each case, would be stable without lateral support. The cross section of each member is so designed that all members will be equally stressed by a normal load at the center of the span and that the total weight of all members will be equal to the total weight of model 1.

48. The number above the line in each case gives the load on the member for one pound normal load at the central span. The number below the line gives the length of the member. In the legend the second column gives the ratio of the section area to the section area of 1 and Column 3 gives the section area in square inches.

49. Plate 13 was added to the report for the purpose of helping to summarize work previously done on aircraft carrier bents. Naval Research Laboratory Report H-1644 shows that for the bents tested much of the web and part of the flanges carried very little load. Failure of the bents tested resulted from warping of the inner flange (p. 11). Bureau of Standards Report R.P. 1161 confirmed this finding. The Bureau of Standards circular flange was built up of two angles rivited together to form the flange. Such a structure has little strength to resist warping forces and failure came, as should have been expected, at a relatively light load. If a knee web is to take the thrust load of the inner flanges a circular flange is a better design than any combination of angles because it gives the most uniform distribution of load from the flange to the web. If a circular flange is used the ratio of width to thickness should be kept low enough so that the thrust of the web will not warp the flange.

CONCLUSIONS FOR MODELS TESTED

50. Model 3 for both C and L proved superior under test to either 1 or 2. Table 2 shows that for stiffness under vertical load 3 is superior to 1 and 2 by 28 and 15.5 per cent respectively. Table 4 shows that for a tangential load these advantages for the hinged end bent are 79 and 43 per cent respectively. These figures represent

the overall stiffness of the different models. They do not directly take into account the local high concentration of web stresses which would be the cause of failure if either 1 or 2 models were overloaded. These local stress concentrations would add another factor in favor of model 3.

51. Diagram A and B of Plate 13 present in simple form the reason why the straight flange model of Bureau of Standards Report R.P. 1224 was superior to the other knees. A straight member is always the best means of carrying load between two points. The Lukenweld model gave the best concentration of metal along the different lines of action of the load. It is interesting to note that in both ideal bents, member 3 carries the greatest load.

52. Diagram A shows that the ideal hinged span support is roughly 57 per cent stronger than model 3 while diagram B shows that the ideal fixed end span would be about 144 per cent stronger.

TABLE I

STATION DISPLACEMENTS DUE TO A FIXED LEG DISPLACEMENT
OF BENT MODELS WITH HINGED ENDS

Model Station	Displace-ment	C. 1	C.2	C.3	L.1	L.2	L.3
0	dH	1.000	1.000	1.000	1.000	1.000	1.000
1	"	.712	.711	.727	.736	.695	.715
2	"	.491	.518	.514	.521	.475	.519
3	dv	.164	.179	.198	.155	.166	.186
4	"	.256	.276	.306	.246	.269	.289
5	"	.296	.319	.334	.275	.300	.340
6	"	.261	.284	.311	.266	.267	.307
7	"	.174	.172	.206	.146	.169	.185
8	dh	.514	.475	.490	..507	.450	.481
9	"	.280	.276	.283	.276	.270	.279

* dh represents horizontal displacements
  dv represents vertical displacements

TABLE 2

MIDSPAN DEFLECTION DUE TO VERTICAL LOADS ON BENT MODELS 'ITH HINGED ENDS

Model Station	Model Load	C-1	C-2	C-3	L-1	L-2	L-3
5	5	.0245	.0209	.0192	.0169	.0132	.0111
5	15	.0729	.0653	.0589	.0496	.0413	.0352
5	35	.1706	.1571	.1388	.1130	.0999	.0847

TABLE 3

CORNER ROTATION DUE TO VERTICAL LOADS ON BENT MODELS WITH HINGED ENDS

Model Station	Model Load	C-1	C-2	C-3	L-1	L-2	L-3
8	5	.00107		.00089	.00081	.00046	.00049
2		.00115	.00091	.000814	.00071	.00033	.00048
8	15	.00322		.00269	.00211	.00157	.00151
2		.00339	.00269	.00249	.00207	.00138	.00145
8	35	.00760		.00620	.00495	.00371	.00368
2		.00768	.00648	.00588	.00489	.00369	.00349

TABLE 4

SIDE SWAY DUE TO LATERAL LOADS ON BENT MODELS WITH HINGED ENDS AND FIXED ENDS

Model Station	Model Load	C-1	C-2	C-3	L-1	L-2	L-3	Displacement
5	5	.0345	.0293	.0105	.0228	.0152	.0138	dh
5	10	.0694	.0611	.0347	.0496	.0349	.0315	dh
		Fixed Ends - Lateral Load						
5	5	.0085	.0084	.0074	.0067	.0054	.0064	dh
5	10	.0171	.0170	.0151	.0137	.0112	.0125	dh
	20	-	-	-	.0287	.0221	.0258	dh

TABLE 5

STATION DISPLACEMENTS DUE TO A FIXED LEG DISPLACEMENT OF BENT MODELS WITH FIXED ENDS

Model Station	C-1	C-2	C-3	L-1	L-2	L-3	Displacement
0	1.000	1.000	1.000	1.000	1.000	1.000	dH
1	.811	.818	.820	.788	.820	.766	dH
2	.517	.561	.550	.522	.525	.498	dH
3	.246	.259	.276	.244	.222	.252	dV
4	.374	.416	.445	.380	.346	.377	"
5	.406	.463	.494	.429	.390	.421	"
6	.361	.420	.428	.382	.307	.384	"
7	.245	.256	.274	.255	.210	.233	"
8	.481	.467	.464	.434	.483	.444	dH
9	.189	.194	.193	.184	.188	.205	dH

TABLE 6

CORNER ROTATION DUE TO A FIXED LEG DISPLACEMENT OF BENT MODELS WITH FIXED ENDS

Model Station	C-1	C-2	C-3	L-1	L-2	L-3
8	no	.0471	.0428	.0398	.0424	.0400
2	data	.0462	.0456	.0420	.0470	.0420

TABLE 7

MIDSPAN DEFLECTION DUE TO VERTICAL LOADS ON BENT MODELS WITH FIXED ENDS

Model Station	Model Load	C-1	C-2	C-3	L-1	L-2	L-3
5	5	.0217	.0200	.0171	.0153	.0135	.0119
5	15	.0659	.0627	.0524	.0467	.0394	.0355
5	35	.1535	.1522	.1281	.1096	.0890	.0835

TABLE 8

RATIO OF STATION DISPLACEMENTS TO A FIXED LEG ROTATION
OF BENT MODELS WITH HINGED ENDS

Model Station	C-1	C-2	C-3	L-1	L-2	L-3
0	0	0	0	0	0	0
1	3.99	5.43	3.87	4.11	3.92	2.55
2	5.49	7.06	4.85	5.76	5.10	3.30
3	- 0.26	- 0.41	- 0.33	- 0.35	- 0.15	- 0.22
4	+ 0.05	- 0.06	+ 0.06	- 0.05	+ 0.25	- 0.04
5	+ 0.45	0.66	0.66	0.41	0.78	0.37
6	1.05	1.47	1.13	1.23	1.13	0.73
7	0.91	1.36	1.03	0.73	0.98	0.74
8	5.21	6.71	4.65	5.52	4.85	3.46
9	3.26	4.38	2.98	3.26	3.05	2.56

TABLE 9

RATIO OF STATION DISPLACEMENTS TO A FIXED LEG ROTATION
OF BENT MODELS WITH FIXED ENDS

Model Station	C-1	C-2	C-3	L-1	L-2	L-3
0		0	0	0	0	0
1		4.31	3.11	3.19	3.15	2.03
2		4.12	3.22	3.61	3.45	1.90
3		- 0.43	- 0.34	- 0.30	- 0.41	- 0.02
4		1.19	0.93	0.82	0.94	0.27
5		1.65	1.31	1.16	1.36	0.56
6		2.16	1.55	1.34	1.61	0.86
7		1.58	1.14	0.99	1.23	0.67
8		3.96	2.73	3.84	2.98	1.76
9		1.80	1.24	1.39	1.34	0.88

TABLE 10

MAXIMUM MIDSPAN FIBER STRESS
DUE TO A 35# LOAD ON BENT MODELS

Model	Midspan Deflection 35# Load	Maximum Fiber Stress	Load to Give a Stress of 2000 #/in^2
		HINGED ENDS	
C-1	.1706"	621 #/in^2	113#
C-2	.1571	598	117
C-3	.1388	566	124
L-1	.1130	754	93
L-2	.0999	714	98
L-3	.0847	667	105
		FIXED ENDS	
C-1	.1535	595	118
C-2	.1522	589	119
C-3	.1281	545	128
L-1	.1096	744	94
L-2	.0890	680	103
L-3	.0835	664	105
IDEAL HINGED			130
IDEAL FIXED			201

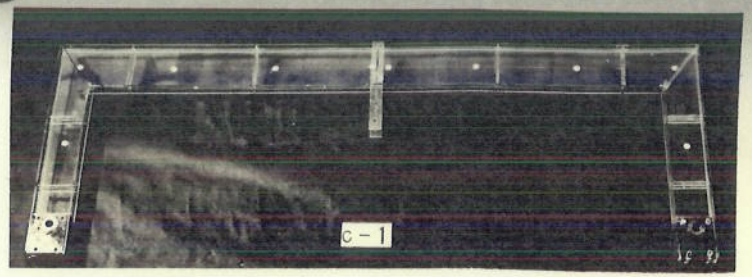

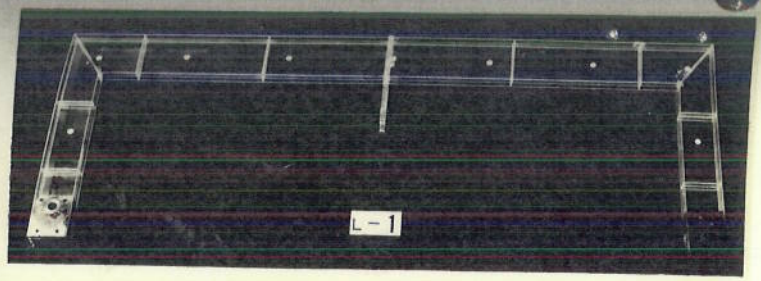

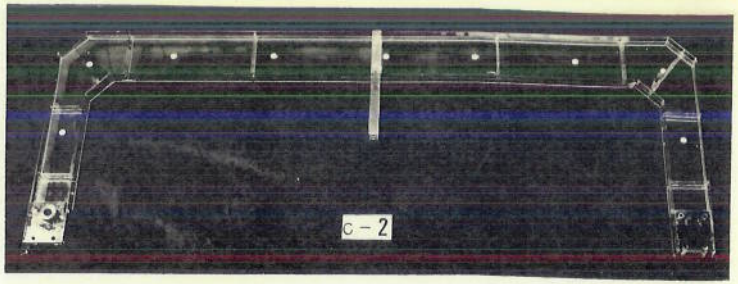

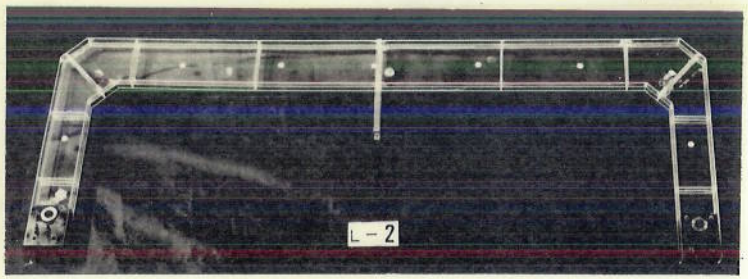

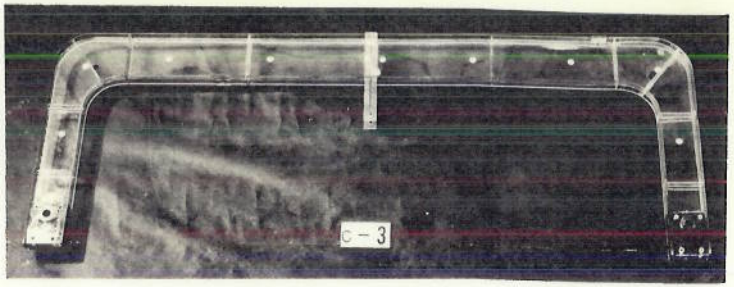

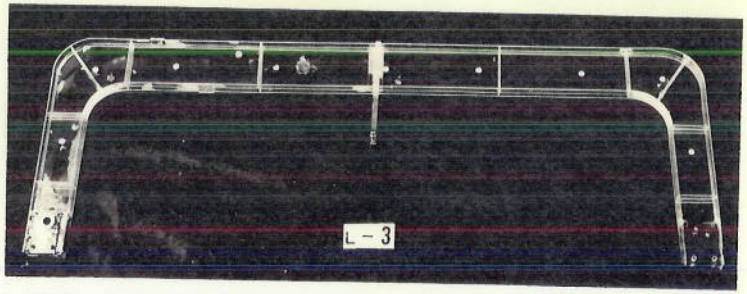

TMB 6364 PLATE 1 10-9-41

PLATE 3

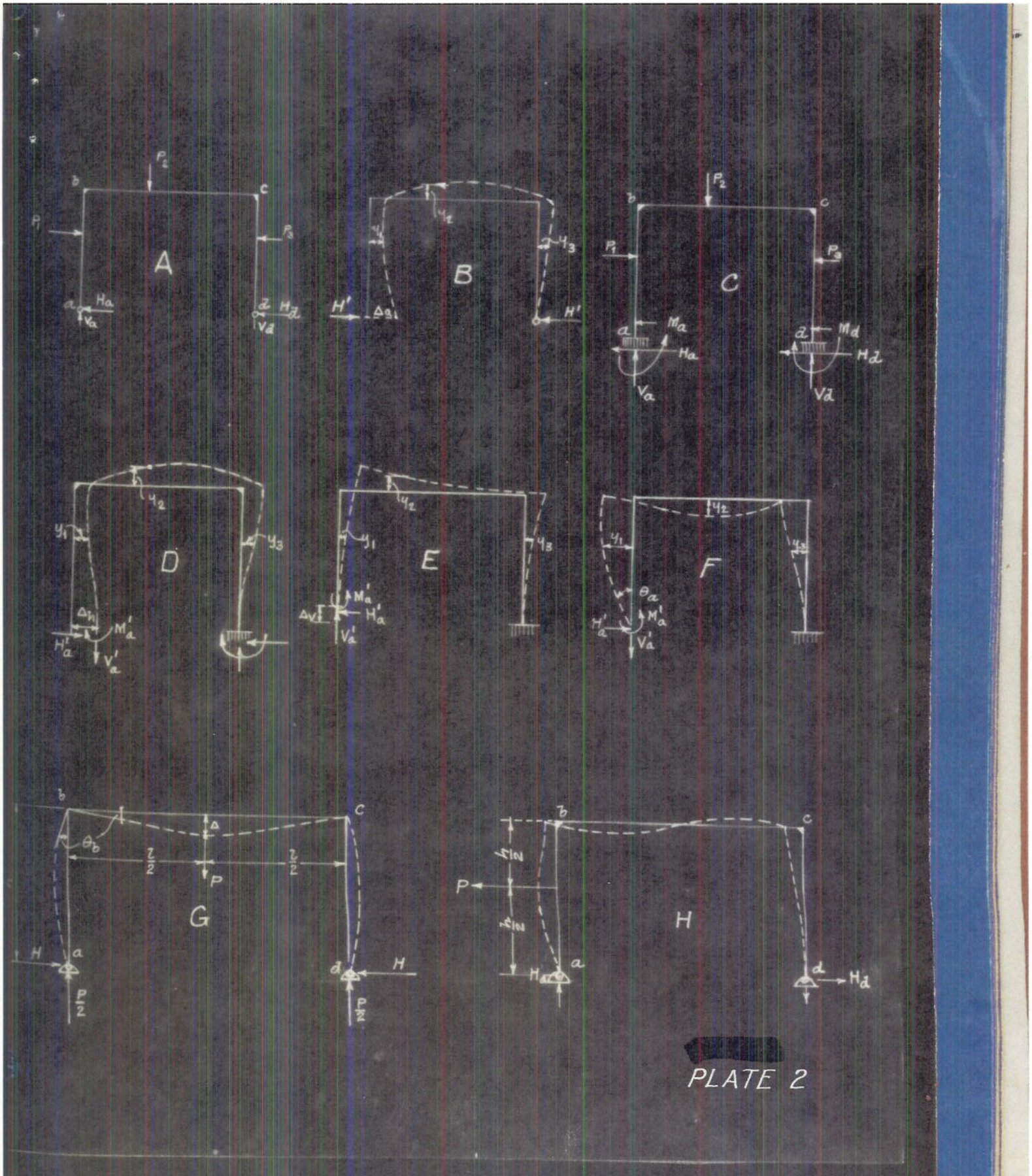

PLATE 3


MODEL C-1

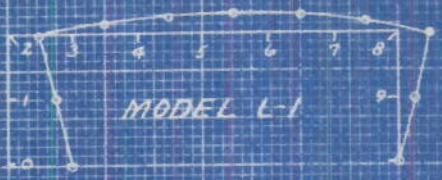
MODEL L-1


MODEL C-2

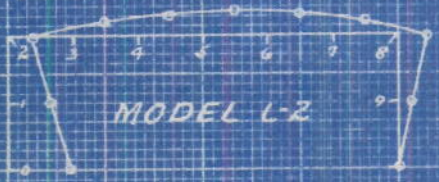
MODEL L-2

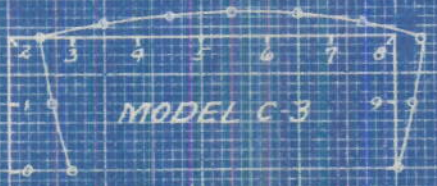
MODEL C-3

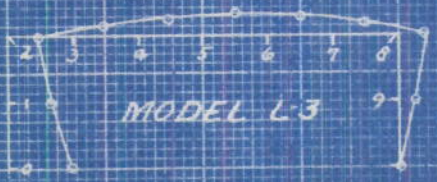
MODEL L-3

H


MODEL C-1


MODEL L-1


MODEL C-2


MODEL L-2


MODEL C-3


MODEL L-3

F

PLATE 3

PLATE 4

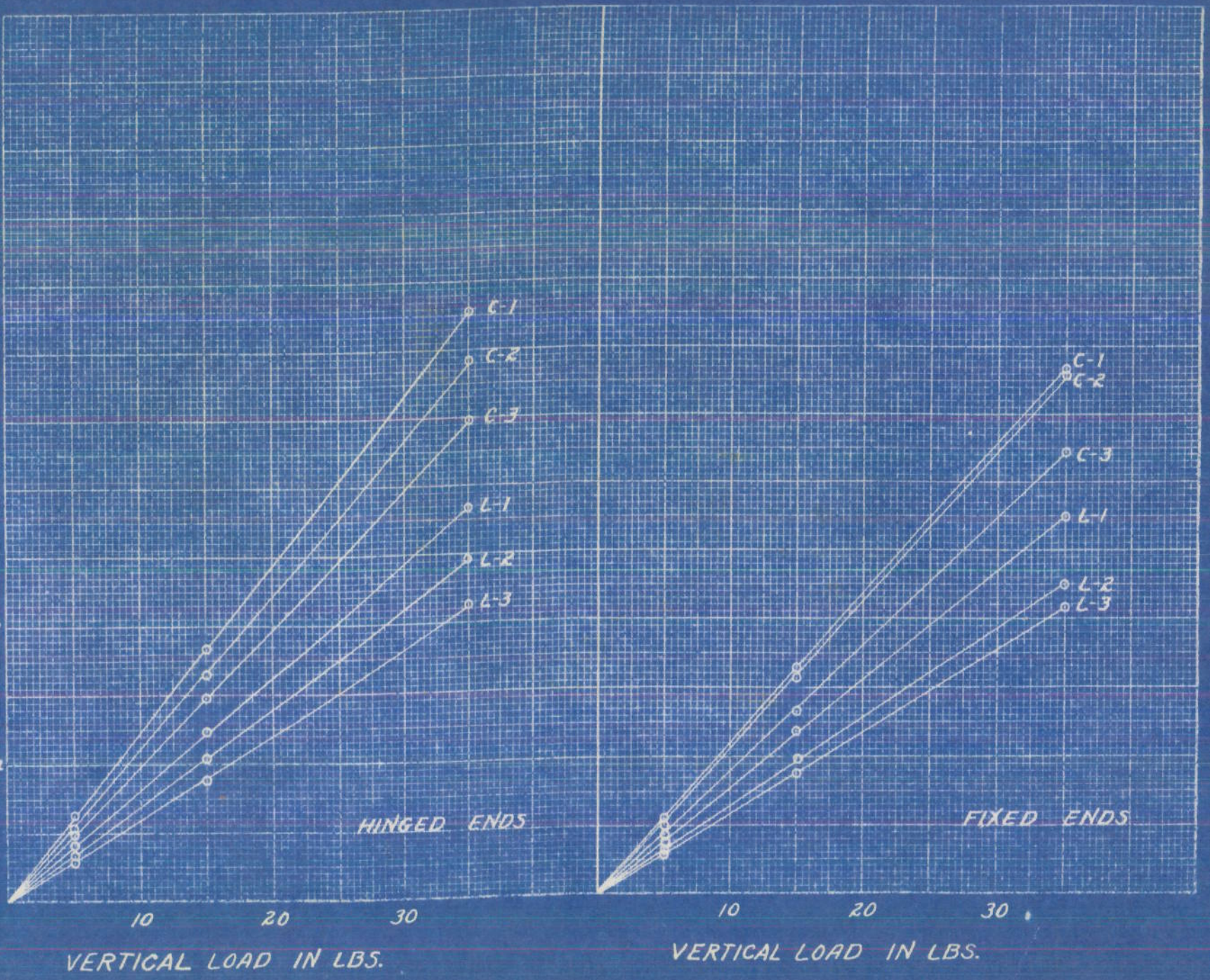
DEFLECTION IN INCHES
.16
.12
.08
.04
C-1
C-2
C-3
L-1
L-2
L-3
HINGED ENDS
10
20
30
VERTICAL LOAD IN LBS.
C-1
C-2
C-3
L-1
L-2
L-3
FIXED ENDS
10
20
30
VERTICAL LOAD IN LBS.

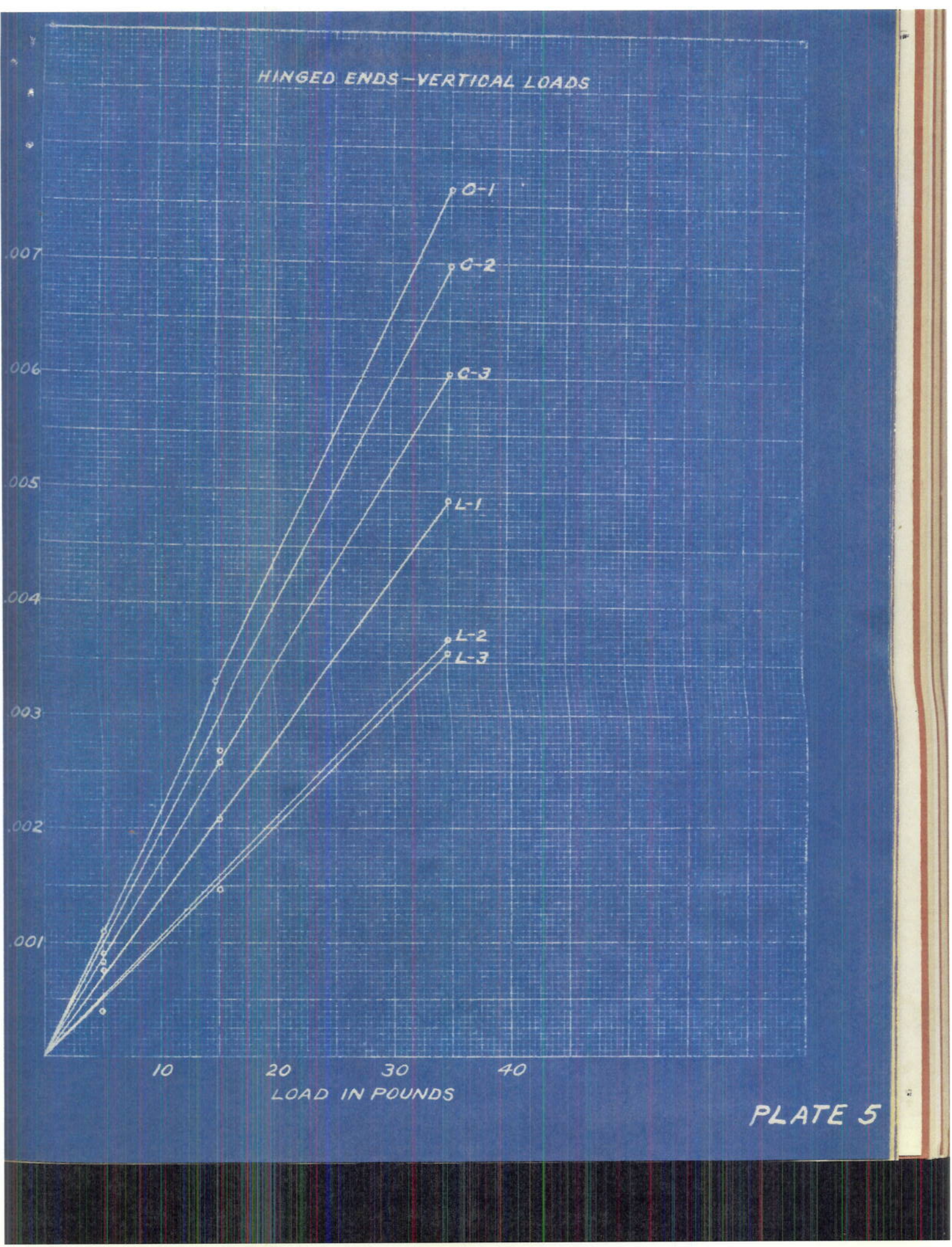
HINGED ENDS—VERTICAL LOADS
C-1
C-2
C-3
L-1
L-2
L-3
.007
.006
.005
.004
.003
.002
.001
10
20
30
40
LOAD IN POUNDS

PLATE 5

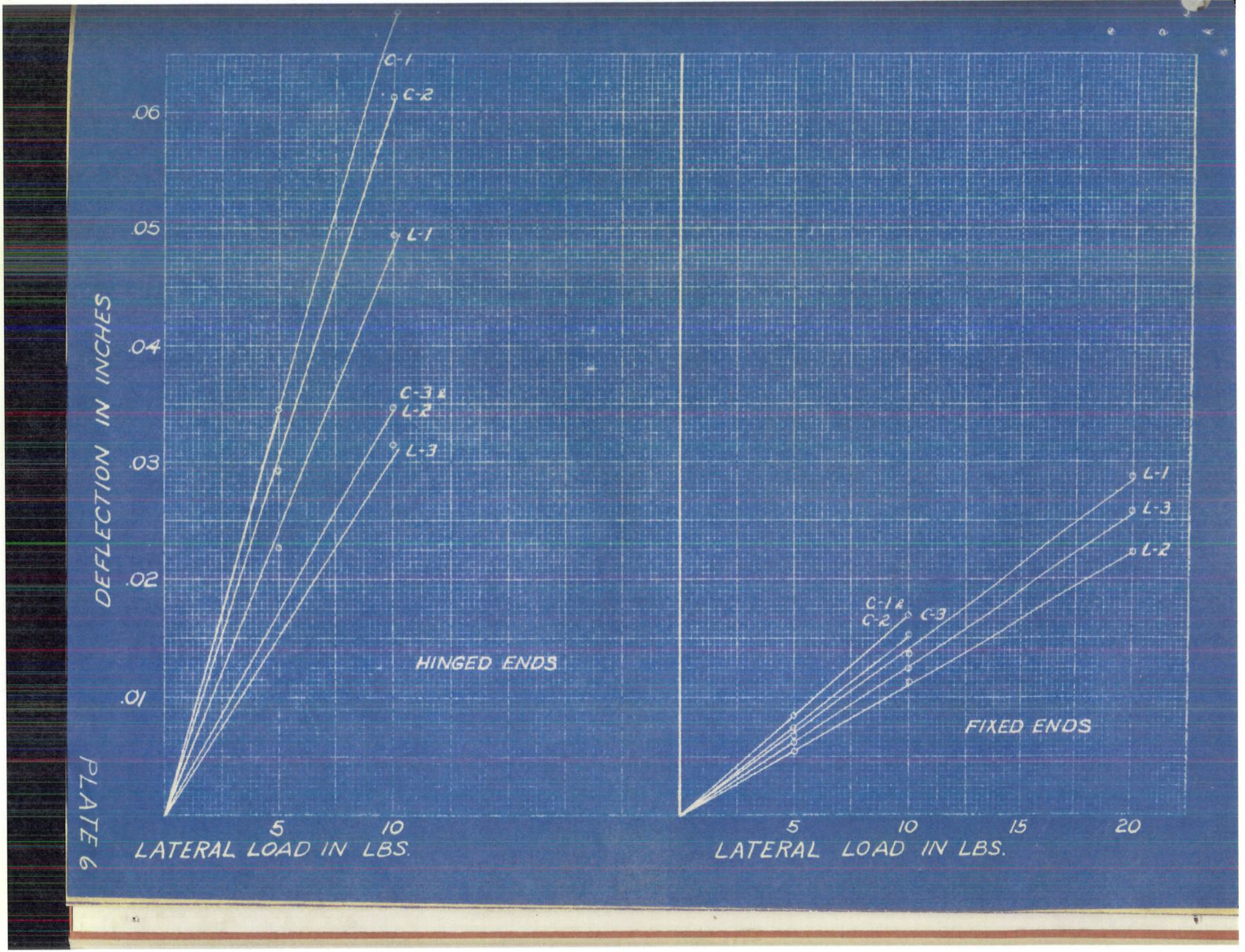
C-1
C-2
L-1
C-3 &
L-2
L-3
.06
.05
.04
.03
.02
.01
DEFLECTION IN INCHES
HINGED ENDS
5
10
LATERAL LOAD IN LBS.
L-1
L-3
L-2
C-1 &
C-2
C-3
FIXED ENDS
5
10
15
20
LATERAL LOAD IN LBS.

PLATE 6

Hinged Ends – Fixed Rotation

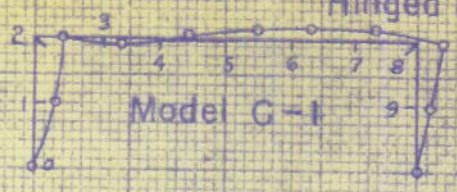

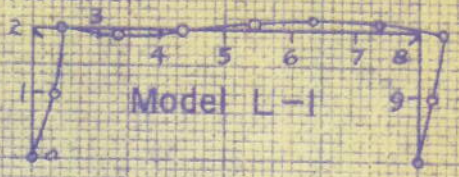

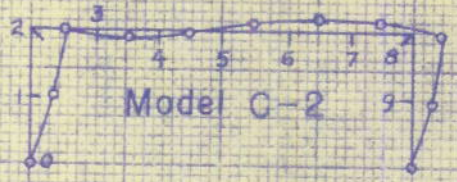

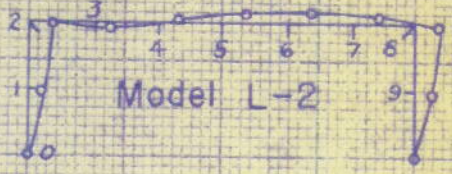

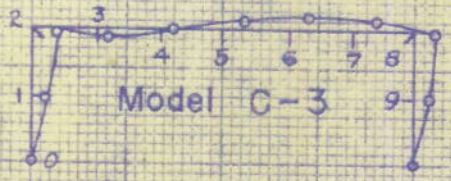

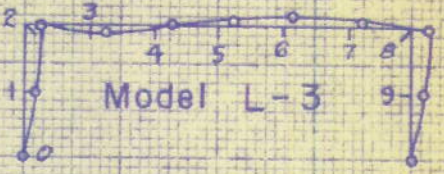

H

Fixed Ends – Fixed Rotation

No Data

Model C-1

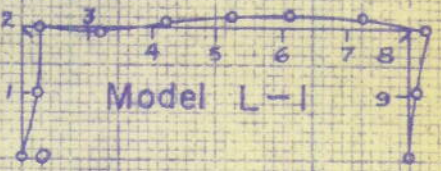

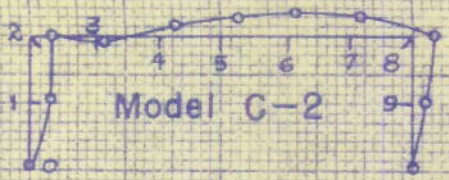

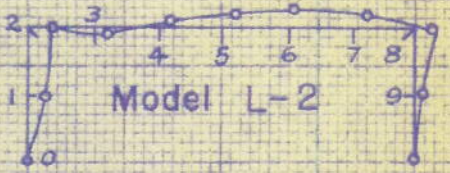

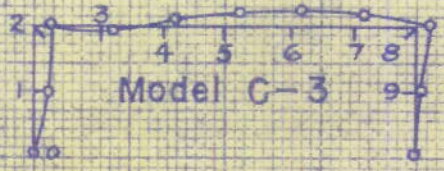

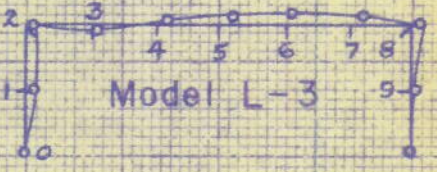

F

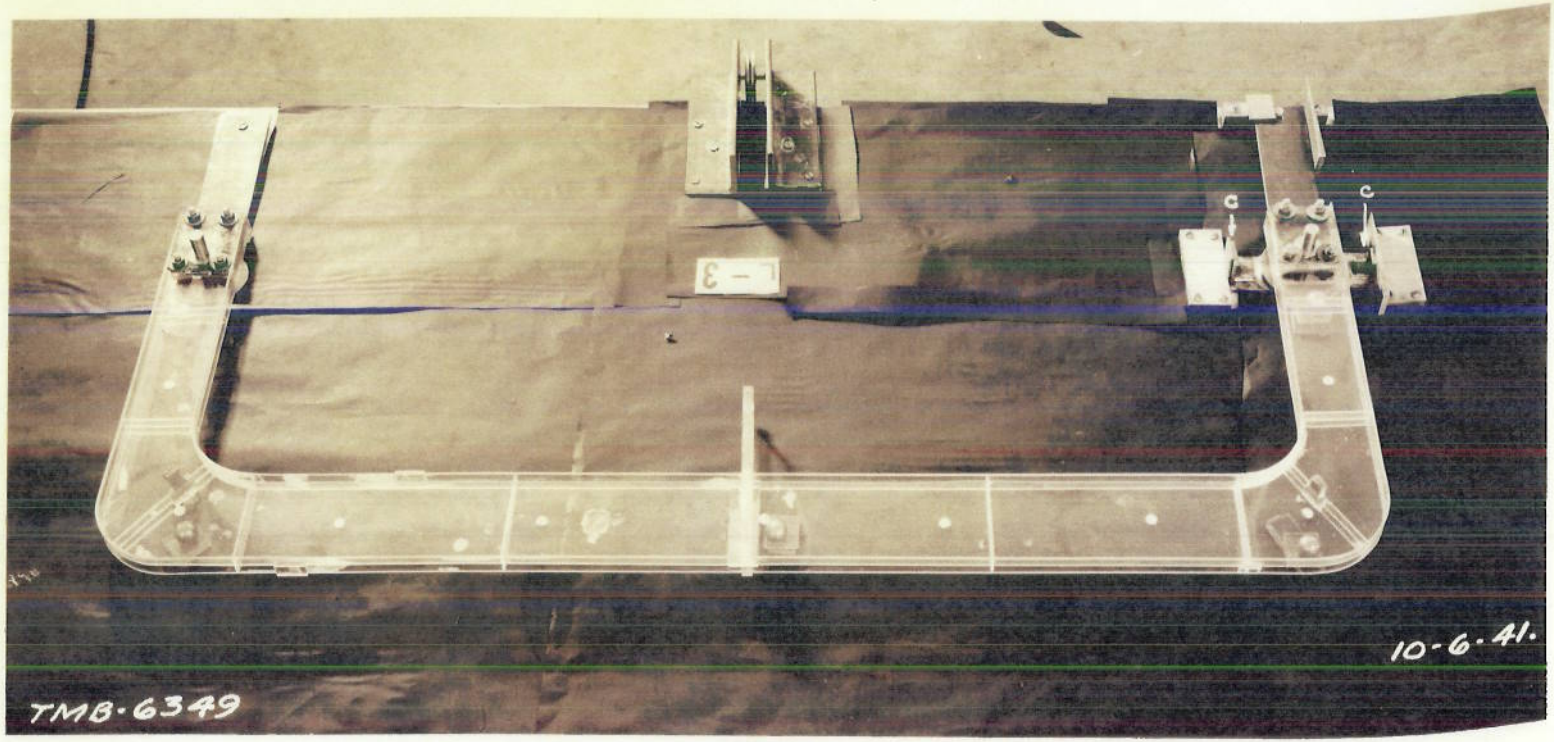

TMB 6349 PLATE 8 10-6-41

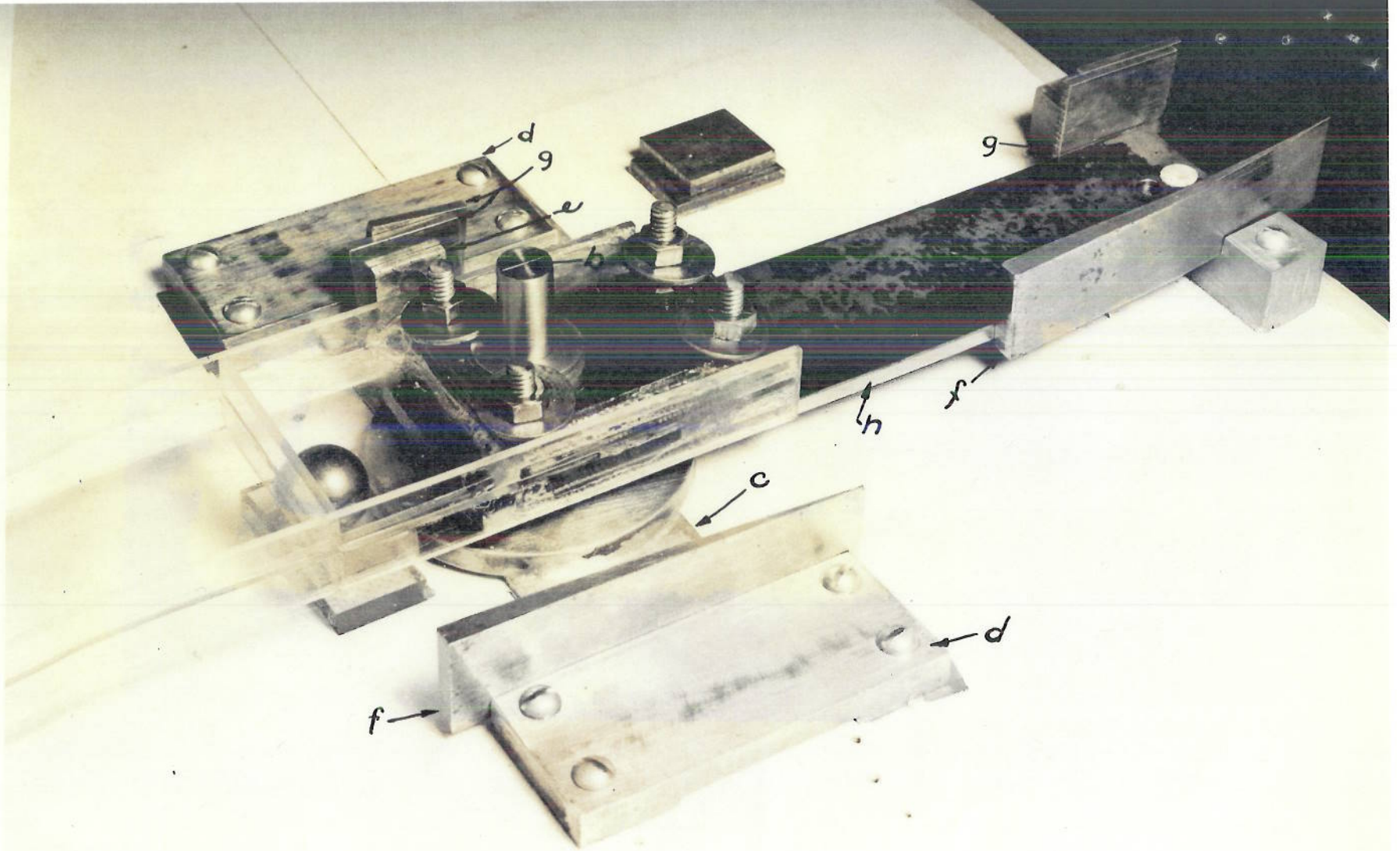

TMB 6347 PLATE 9 10-3-41

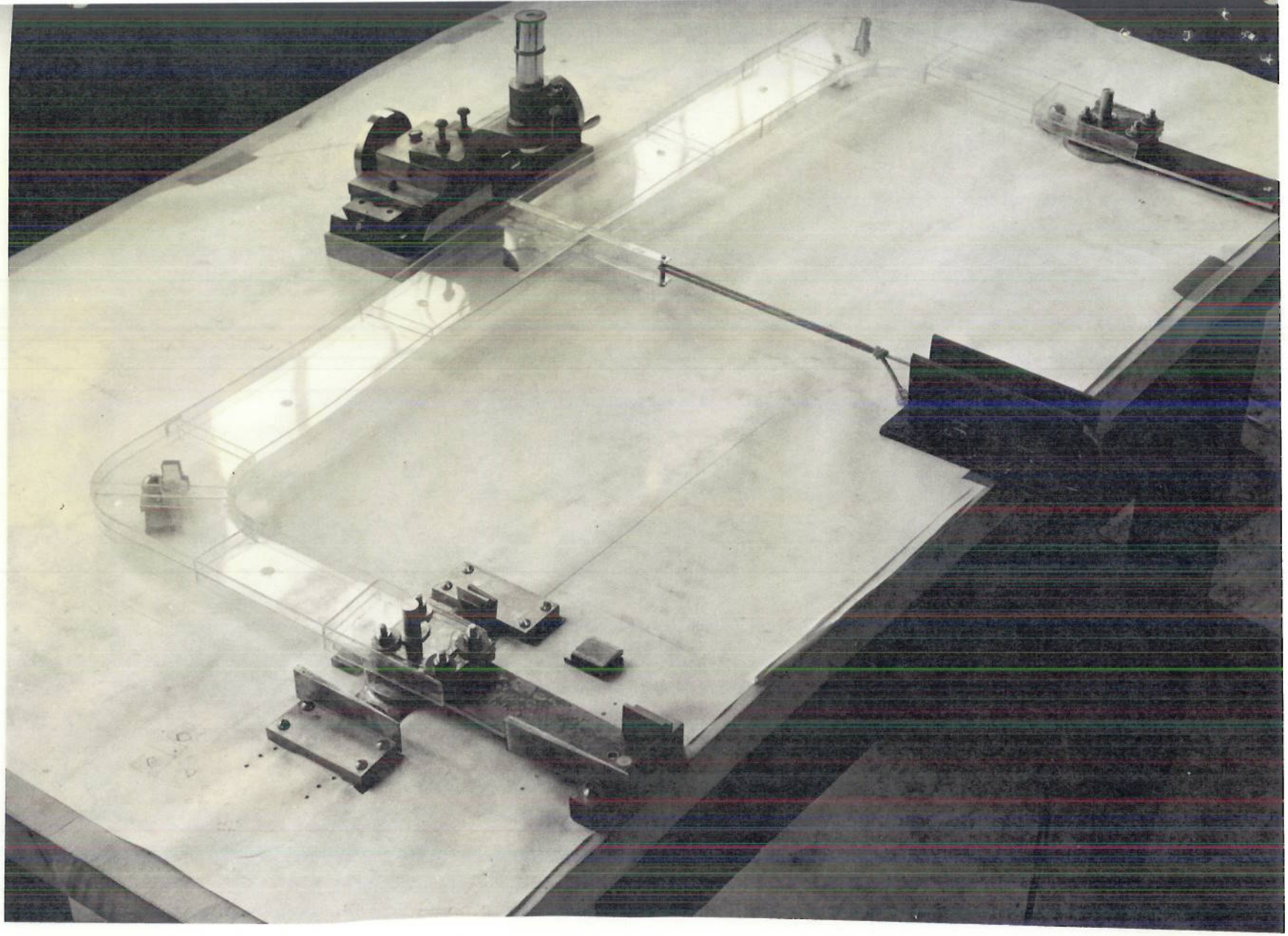

TMB 6348

PLATE 10

10-3-41

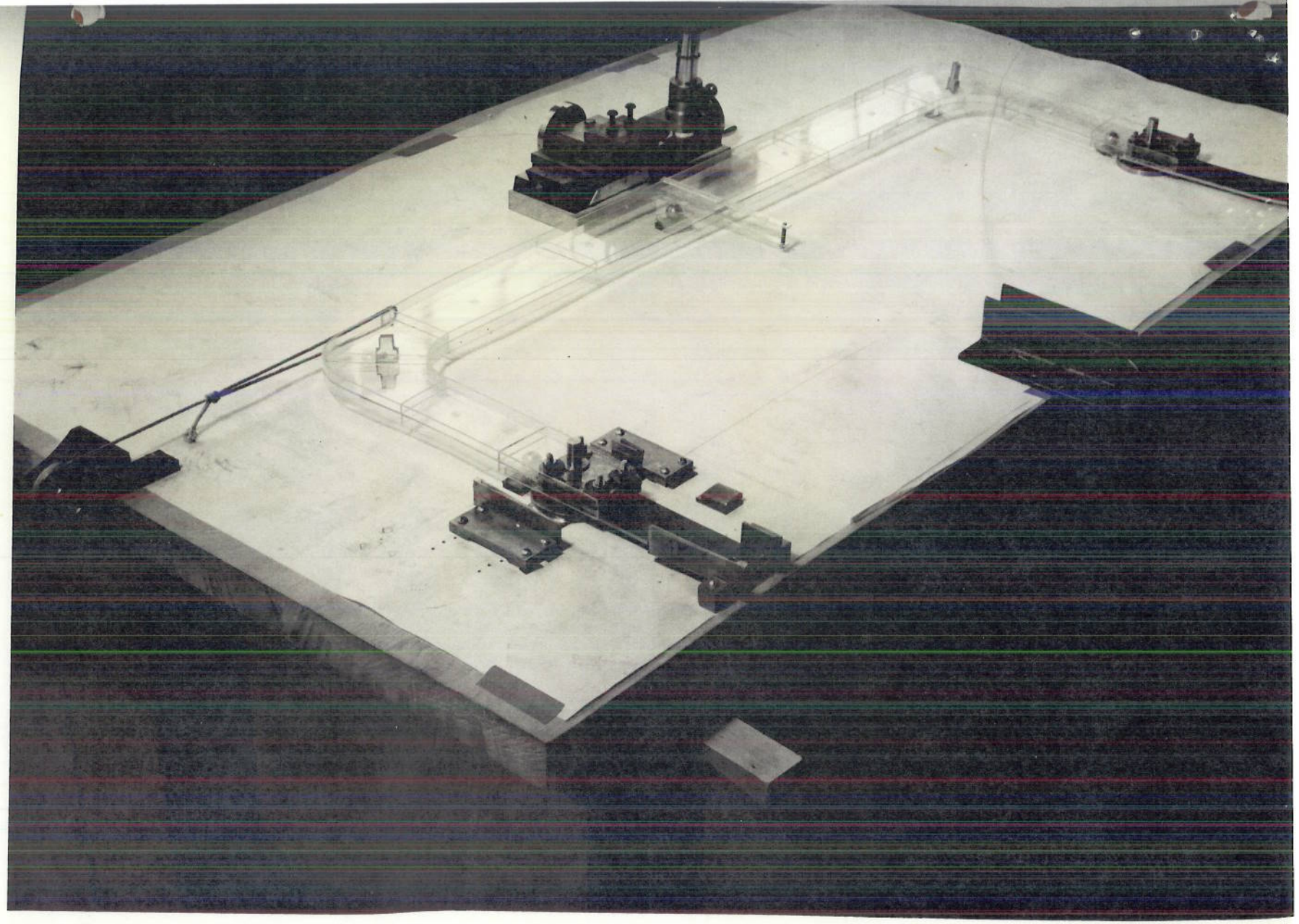

TMB 6346 PLATE 11 10-3-41

509#

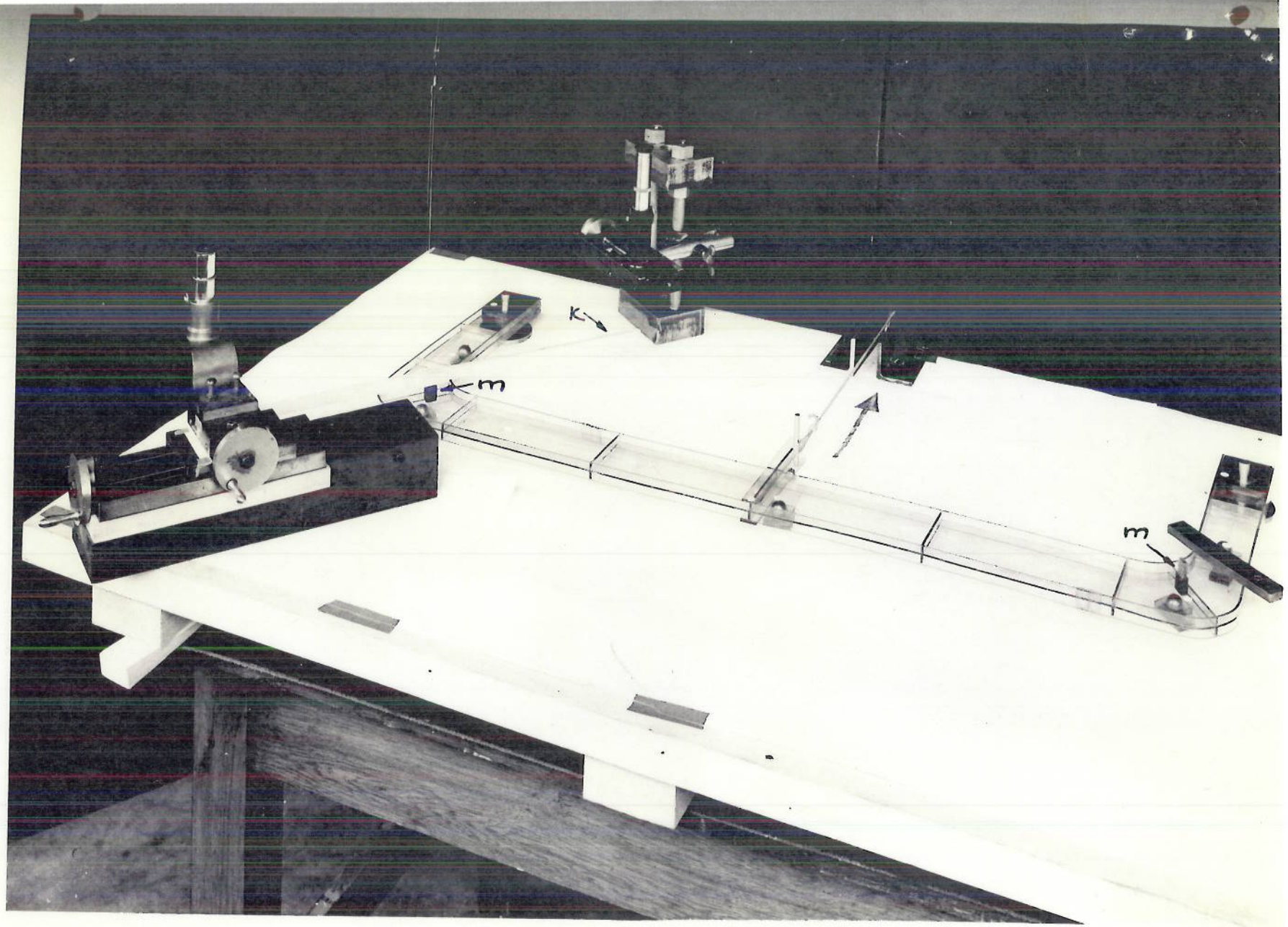

TMB 6340

PLATE 12

9-24-41

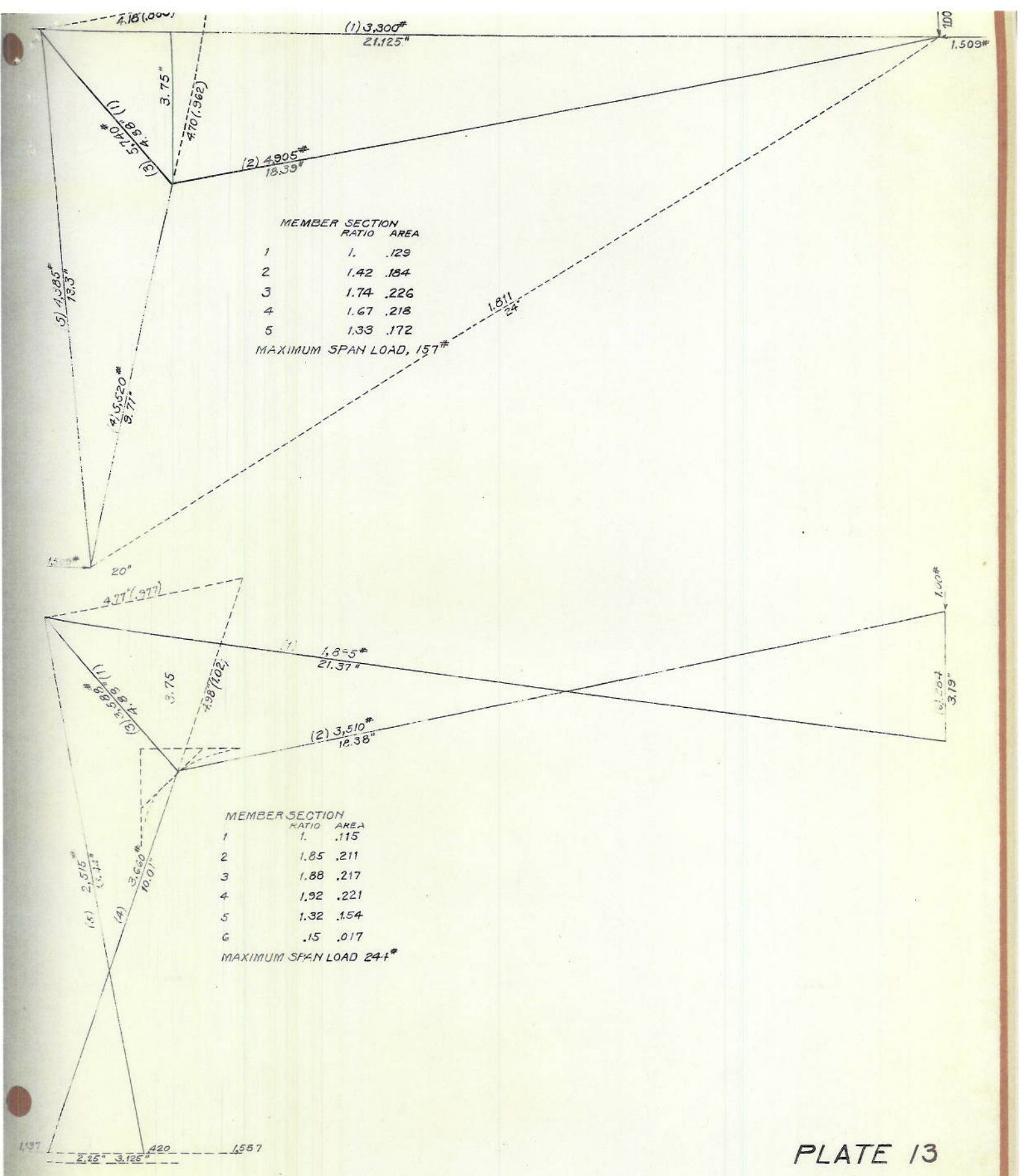
(1) 3,300#
21.125"
1.509#
3.75"
.470(.962)
(3) 5,740#
(2) 4,905#
18.39"
MEMBER SECTION
RATIO AREA
1 1. .129
2 1.42 .184
3 1.74 .226
4 1.67 .218
5 1.33 .172
MAXIMUM SPAN LOAD, 157#
(5) 4,385#
12.3"
4,5520#
3.77"
1.611
24"
20"
4.11"(.977)
(1) 1,855#
21.37"
3.75
.398(1.02)
(3) 3,510#
(2) 3,510#
18.38"
3.19"
MEMBER SECTION
RATIO AREA
1 1. .115
2 1.85 .211
3 1.88 .217
4 1.92 .221
5 1.32 .154
6 .15 .017
MAXIMUM SPAN LOAD 241#
(5) 2,515#
(4) 3,660#
10.01"
1,137
420
1,557
2.25"
3.125"

PLATE 13